The International Journal of Biochemistry & Cell Biology 41 (2009) 2493–2502

Contents lists available at ScienceDirect

The International Journal of Biochemistry & Cell Biology

journal homepage: www.elsevier.com/locate/biocel

# The resveratrol analogue 4,4′-dihydroxy-trans-stilbene inhibits cell proliferation with higher efficiency but different mechanism from resveratrol

M. Savio[a], T. Coppa[a], L. Bianchi[a], V. Vannini[a], G. Maga[b], L. Forti[c], O. Cazzalini[a], M.C. Lazzè[a], P. Perucca[a], E. Prosperi[b], L.A. Stivala[a,*]

[a] Dipartimento di Medicina Sperimentale, sez. Patologia Generale, Università di Pavia, Italy
[b] Istituto di Genetica Molecolare del CNR (IGM-CNR), Pavia, Italy
[c] Dipartimento di Chimica, Università di Modena e Reggio Emilia, Italy

ARTICLE INFO

*Article history:*
Received 15 May 2009
Received in revised form 15 July 2009
Accepted 1 August 2009
Available online 11 August 2009

*Keywords:*
Resveratrol
4,4′-Dihydroxy-trans-stilbene
Cell proliferation
DNA synthesis
DNA polymerases

ABSTRACT

Resveratrol (3,4′,5-trihydroxy-trans-stilbene) is a natural phytoalexin found in grapes and wine, which shows antiproliferative activity. We previously found that 4-hydroxy group in the trans conformation was absolutely required for the inhibition of cell proliferation. In the present work we have synthesized the resveratrol analogue 4,4′-dihydroxy-trans-stilbene, which contains two OH in 4′ and 4 positions, with the aim of developing a compound with an antiproliferative potential higher than that of resveratrol, on the basis of the correlation between structure and activity previously observed. In comparison with resveratrol, 4,4′-dihydroxy-trans-stilbene inhibited cell clonogenic efficiency of fibroblasts nine times more although with a different mechanism. First, 4,4′-dihydroxy-trans-stilbene induced predominantly an accumulation of cells in G1 phase, whereas resveratrol perturbed the G1/S phase transition. Second, although both compounds were able to inhibit DNA polymerase (pol) δ in an in vitro assay, 4,4′-dihydroxy-trans-stilbene did not affect pol α activity. Finally, 4,4′-dihydroxy-trans-stilbene increased $p21^{CDKN1A}$ and p53 protein levels, whereas resveratrol led to phosphorylation of the S-phase checkpoint protein Chk1. Taken together, our results demonstrated for the first time that the two hydroxyl groups on 4- and 4′- positions of the stilbenic backbone enhance the antiproliferative effect and introduce additional targets in the mechanism of action of resveratrol. In conclusion, 4,4′-dihydroxy-trans-stilbene has potent antiproliferative activities that differ from the effect of resveratrol shown in this system, suggesting that it warrants further development as a potential chemopreventive or therapeutic agent.



## 1. Introduction

Stilbenes are naturally occurring compounds that act as protective agents to defend plants against adverse conditions such as viral and microbial attack or environmental stress (Langcake and Pryce, 1977; Hain et al., 1990; Soleas et al., 1997). Among the stilbenic compounds, the 3,5,4′-trihydroxy-trans-stilbene, known as resveratrol (RSV), is found mainly in grapes and red wine. The interest in this molecule has increased exponentially in the last 10 years, following the major findings showing that it can prevent or delay a wide variety of human pathological processes, including inflammation (Kimura et al., 1985; Rotondo et al., 1998; Jang et al., 1999), cardiovascular diseases (Pace-Asciak et al., 1995, 1996; Klinge et al., 2008), and cancer (Jang et al., 1997; Mgbonyebi et al., 1998; Hsieh et al., 1999b). In addition, RSV seems to be effective in increasing the lifespan of various organisms, from yeast to small mammals (Howitz et al., 2003; Baur et al., 2006; Barger et al., 2008) and in delaying the onset of a variety of age-related diseases, such as diabetes (Milne et al., 2007). The mechanism by which RSV exerts such a range of beneficial effects is not yet clear, and multiple direct targets have been identified for this small natural compound. RSV displays antioxidant properties (Frankel et al., 1993; Kerry and Abbey, 1997), anti-cyclooxygenase activity (Jang et al., 1997; MacCarrone et al., 1999; Szewczuk et al., 2004) and a modulating effect on lipid and lipoprotein metabolism (Arichi et al., 1982; Kimura et al., 1985; Goldberg et al., 1995). RSV also inhibits ribonucleotide reductase (Fontecave et al., 1998), and DNA polymerases (Sun et al., 1998; Stivala et al., 2001; Locatelli et al., 2005), and it interferes with the mitogen-activated protein kinase and protein kinase C pathways (Pace-Asciak et al., 1996; Kotha et al., 2006). Finally, RSV is a potent activator of sirtuin activity, and mimics the beneficial effects of caloric restriction (Baur et al., 2006; Barger et al., 2008).

* Corresponding author at: Dipartimento di Medicina Sperimentale, Sez. Patologia Generale, Piazza Botta 10, 27100 Pavia, Italy. Tel.: +39 0382 986397; fax: +39 0382 303673.
*E-mail address:* luciaanna.stivala@unipv.it (L.A. Stivala).

1357-2725/$ – see front matter © 2009 Elsevier Ltd. All rights reserved.
doi:10.1016/j.biocel.2009.08.005

Our previous study, aiming to explain the relationship between chemical structure and biological activity of RSV, showed that the 4′-hydroxystyryl moiety was absolutely required for the antiproliferative activity and the DNA polymerase inhibition (Stivala et al., 2001). In order to enhance these effects, we modified the molecule by introducing two hydroxyl groups in 4,4′ positions, resulting in the RSV analogue, 4, 4′-dihydroxy-trans-stilbene (DHS). Antioxidant and antiestrogenic activity of DHS have been previously investigated (Cai et al., 2003; Balan et al., 2006). In particular, it has been demonstrated that DHS acts as an effective antioxidant against linoleic acid peroxidation and free-radical-induced peroxidation of rat liver microsomes (Fang et al., 2001, 2002), and of human low-density lipoprotein (Cheng et al., 2006). More recently, a limited number of studies have shown that it acts as a specific estrogen receptor (ER) ligand, with a binding affinity much higher than that of other well-known ER agonists (Balan et al., 2006). In contrast, no data are available about the effect of DHS on cell proliferation. In the present study, we have investigated whether DHS shows antiproliferative effects similar to those of RSV. In particular, we first assessed the effects on cell proliferation by analyzing the cell clonogenic efficiency and cell cycle progression, using primary human fibroblasts. Then, we have evaluated the ability of DHS to inhibit in vitro replicative DNA polymerases. Finally, to elucidate the mechanism of action on cell cycle progression, we investigated the effects of DHS on the expression and levels of cell cycle regulatory proteins.

## 2. Materials and methods

### 2.1. Reagents

trans-Resveratrol and all other chemicals of reagent grade were obtained from Sigma. trans-4,4′-dihydroxystilbene was obtained by Perkin condensation as previously described (Locatelli et al., 2005).

### 2.2. Cell culture and treatments

LF1 human lung fibroblasts (gift from J. Sedivy, Brown University Providence, RI), were cultured in MEM medium (Invitrogen), supplemented with 10% fetal bovine serum, 100 IU/ml penicillin and 100 μg/ml streptomycin. LF1 were used between the 5th and 20th passages. Cell treatments were performed by adding RSV or its analogue in culture medium, at final concentrations ranging from 1 to 90 μM for 24 h. Both compounds were dissolved in dimethylsulphoxide (DMSO) never exceeding 0.1% in culture medium.

### 2.3. MTT and clonogenic efficiency assays

Cell toxicity was determined by the 3-[4,5-di-methylthiazol-2-yl]-2,5-diphenyl-tetrazoliumbromide (MTT) assay (Mosmann, 1983). Cells were incubated for 24 h with each compound at the following concentrations: 1, 2.5, 5, 7.5, 15, 30, 60, 90 μM. At the end of the treatment, 0.9 mM MTT was added to the medium in each well. After 2 h incubation at 37 °C, the medium was removed, the precipitate blue formazan dissolved in 1 ml DMSO, and immediately quantified by absorption measurements at 570 nm using a microtiter plate reader (Biorad). Cell toxicity was calculated measuring the difference in optical density of treated samples with respect to control and DMSO-treated cells.

The clonogenic efficiency was determined as previously described (Stivala et al., 2001). DHS or RSV was added to the medium at the same concentrations used for MTT assay. The clonogenic efficiency was calculated as the mean percentage with respect to control and DMSO-treated cells. The effective concentration giving 50% inhibition ($IC_{50}$) was calculated from the inhibition curve. DMSO did not affect cell viability or cell clonogenic efficiency of LF1 cells in all the experiments performed.

### 2.4. Cell cycle analysis

For the analysis of DNA content, LF1 were treated for 24 h with 7.5, 15, 30 μM RSV or DHS. At the end of incubation, cells were trypsinized, washed in PBS, and resuspended in PBS containing 100 μg/ml RNase A, 0.05% NP-40 and 5 μg/ml propidium iodide (PI). Staining occurred for at least 30 min at room temperature (r.t.). Ten thousand cells were analyzed for each sample with a Coulter Epics XL flow cytometer (Stivala et al., 2001).

### 2.5. BrdU immunofluorescence

LF1 cells were treated with RSV or DHS for 24 h, at a concentration ranging from 2.5 to 30 μM. During the last hour of culture, cells were incubated with 30 μM BrdU as previously described (Alessi et al., 1998). Visualization was performed with an Olympus BX51 fluorescence microscope, equipped with a C4040 digital camera.

### 2.6. DNA polymerase assays

Pol α, pol β and pol δ activities were assayed as previously described (Stivala et al., 2001). For the inhibition assays, 20 μM of the inhibitors to be tested were added to the reaction mixture in the absence of DNA template and nucleotides. After 5 min of incubation at r.t., the reaction was started by addition of the missing reagents.

### 2.7. In vitro DNA synthesis reaction

In vitro DNA synthesis was performed on HeLa isolated nuclei as described (Krude, 2000). 1 μl of nuclei were incubated for 2 h at 37 °C in a volume of 13 μl of HeLa S-phase cytosolic extract, supplemented with ATP and ATP-regenerating system (40 mM HEPES, pH 7.8, 7 mM $MgCl_2$, 3 mM ATP, 0.1 mM of each GTP, CTP and UTP, 0.1 mM of each dATP, dCTP, and dGTP, 0.5 mM DTT, 40 mM creatine phosphate, all from Roche Applied Science), 2 μg of creatine phosphokinase (Calbiochem), 0.25 μM biotin-16dUTP, in the presence or in the absence of 1 mM RSV or DHS. Reactions were stopped with 100 μl of 0.5% Triton X-100 and nuclei were fixed by adding 100 μl of 8% paraformaldehyde. After 5 min at r.t., nuclei were overlaid on 1 ml of 30% sucrose onto polylysine-coated coverslips, and then were labelled with streptavidin-Texas red (Amersham) for 30 min at 37 °C, counterstained with Hoechst 33258 and mounted in Mowiol. Microscopy visualization was performed as indicated above.

### 2.8. Pathway-specific gene microarray

Total RNA was isolated from LF1 cells treated with RSV or DHS and a cell cycle pathway-specific genes were detected using a GEArray human cell cycle gene array, and a GEArray chemiluminescence detection kit (SuperArray Bioscience Corporation, Frederick, MD). Briefly, 3 μg of total RNA was used for reverse transcription reaction to obtain cDNA. The cDNA probe was labelled with biotin-16-dUTP using a probe synthesis kit from SuperArray. After pre-hybridization, the membrane was hybridized with the labelled cDNA probe overnight with agitation at 5–10 rpm. The imaging of the gene expression was obtained through chemiluminescent detection, after binding alkaline phosphatase-conjugated streptavidin to the hybridized membrane. Data acquisition and analysis on computer were completed by the use of gene analysis software (GEArray Expression Analysis Suite) provided by SuperArray.

### 2.9. Cell extraction procedures and Western blot analysis

For total content determination of proteins, cells were directly lysed in loading buffer and boiled. For analysis of chromatin-bound proteins, cells were lysed in hypotonic buffer (10 mM Tris–HCl, pH 7.4, 2.5 mM $MgCl_2$, 0.5% Nonidet NP-40) containing 1 mM PMSF, 0.2 mM $Na_3VO_4$ and protease and phophatase inhibitor cocktails. After 8 min on ice, cells were pelletted at 200 g, and the detergent-soluble fraction was recovered. Lysed cells were washed in hypotonic buffer and chromatin-bound proteins released with DNAse I, as described (Scovassi and Prosperi, 2006). Whole and fractionated cell extracts were resolved on SDS-PAGE gradient gels, transferred to nitrocellulose membranes, probed with specific antibodies and revealed using enhanced chemiluminescence (Amersham).

Membranes were probed with anti-p21 (CP74, Neomarkers), anti-p27 (Becton Dickinson), anti-p16 (Santa Cruz Biotechnology), anti-cyclin D (Upstate), anti-MCM2 and anti-pRb (BD Biosciences), anti-cyclin A, anti-p53 and anti-actin (Sigma) antibodies.

### 2.10. Flow cytometry and immunofluorescence analysis of MCM2

Treatments were performed on proliferating cells, or on cells synchronized in G0/G1 by 72 h of serum deprivation. After 24 or 48 h of treatments with RSV or DHS, cells were detached by trypsin and lysed at 4 °C in a hypotonic buffer as indicated above. Thereafter, samples were washed once in hypotonic buffer, fixed in 1% formaldehyde for 5 min, and then post-fixed in 70% ethanol. After rehydration, samples were blocked in PBA (PBST + 1% bovine serum albumin), and then incubated for 1 h with anti-MCM2 monoclonal antibody, diluted 1:100 in PBA buffer. After three washes in PBST (PBS + 0.2% Tween 20) buffer, samples were incubated for 30 min with Alexa Fluor-488 conjugated anti mouse antibody (Molecular Probes) diluted 1:200 in PBA. After immunoreactions, samples were incubated for 30 min with 20 μg/ml PI in PBS containing 1 mg/ml RNase A, and then cells were analyzed by flow cytometry as indicated above.

### 2.11. Statistical analysis

Data are presented as means ± SD. Statistical analysis was performed by the Student *t*-test. Probability values $p < 0.05$ were considered to be statistically significant.

## 3. Results

Fig. 1 shows the chemical structure of 3,4′,5-trihydroxy-trans-stilbene (RSV) and its synthetic analogue 4,4′-dihydroxy-trans-stilbene (DHS).

### 3.1. DHS caused cytotoxic effect and cell growth inhibition in normal human fibroblasts

To examine the antiproliferative potential of the synthetic RSV analogue, its effect on cell proliferation was investigated in LF1 human fibroblasts. Exponentially growing LF1 were treated with concentrations of RSV or DHS ranging from 1 to 90 μM. The cytotoxicity was measured by the MTT assay after 24-h treatment with each compound. RSV did not significantly affect cell growth and survival up to 60 μM, whereas a 30% reduction of living cells was observed at the highest concentration used (Fig. 2A). When compared to RSV, DHS was found to be more effective. In fact, it induced a cytotoxic effect by about 35% at 15 μM, and by about 50% at 90 μM. Next, the growth inhibition of RSV and DHS was evaluated by determining the clonogenic efficiency of LF1. Despite the close structure similarity with RSV, DHS exhibited stronger antiproliferative activity

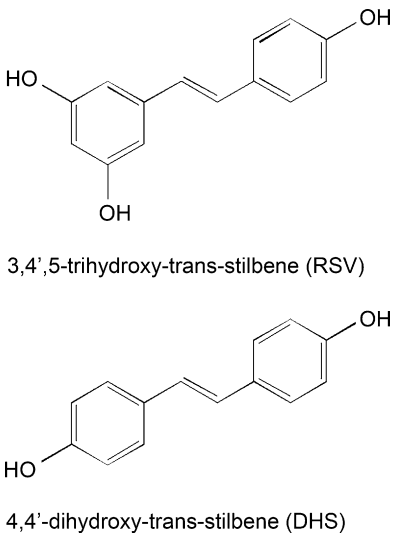


**Fig. 1.** Chemical structures of trans-resveratrol (RSV) and trans-dihydroxystilbene (DHS).

in this assay. Both compounds showed concentration-dependent reduction in clonogenic efficiency of cells, but DHS was more effective than RSV (Fig. 2B), giving $IC_{50}$ that was nine times lower than that of RSV (5 versus 45 μM, $p < 0.01$). Based on the above results, further experiments were performed with drug concentrations inducing comparable effect on cell toxicity and proliferation, i.e. 2.5 and 7.5 μM of DHS against 30 μM of RSV.

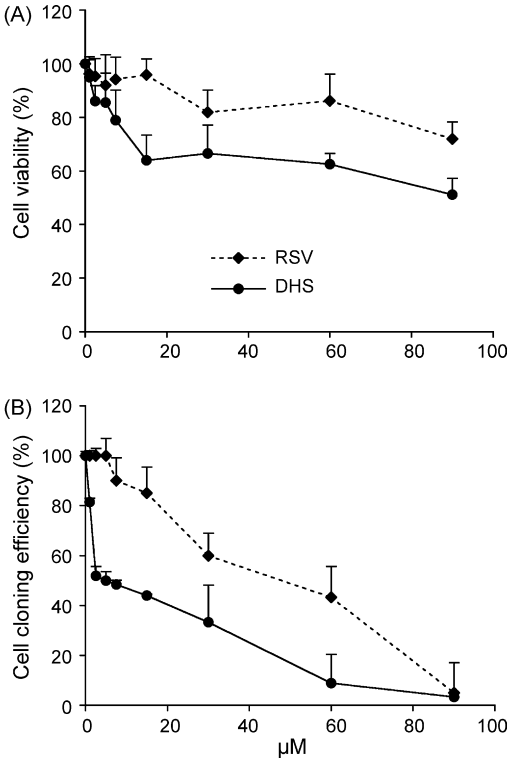


**Fig. 2.** Effect of RSV and DHS on cell survival and proliferation of human fibroblasts. Cell viability (A) and cell clonogenic efficiency (B) evaluated in LF1 primary human fibroblasts after 24 h of treatment with increasing concentrations of RSV or DHS. The percentage of viable cells and clonogenic survival was calculated measuring the difference in optical density or colonies formation, respectively, with respect to control and vehicle-treated cells (0.1% of DMSO), as described in Section 2. All results are expressed as mean ± SD from three independent experiments.

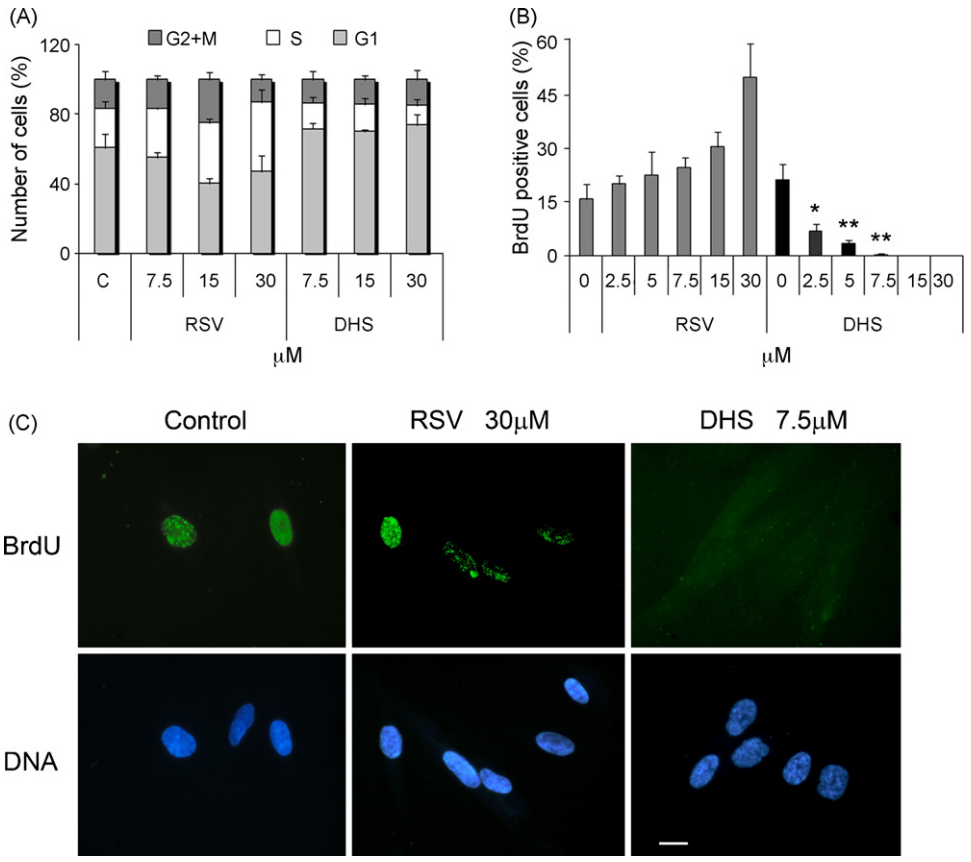


**Fig. 3.** Effect of RSV and DHS on cell cycle progression of human fibroblasts. Cell cycle phase distribution (A) of LF1 primary human fibroblasts after 24 h of treatment with different concentrations of RSV and DHS. Cells were then fixed and the DNA content determined by flow cytometric analysis, as described in Section 2. Effect on DNA synthesis (B) evaluated by BrdU incorporation in fibroblasts seeded on coverslips, and treated with increasing concentration of RSV and DHS, as described in Section 2. All results are expressed as mean ± SD from three independent experiments, and representative images of BrdU-positive cells are showed in the panel C. Scale bar 10 μM. $^{*}p \leq 0.05$, $^{**}p \leq 0.01$.

### 3.2. DHS arrests the cells at the G1 phase of the cell cycle

To better analyze the observed cell cycle imbalance induced by RSV and DHS, the distribution in each phase of the cell cycle was analyzed by determining DNA content with flow cytometry. Fig. 3A compares the effect on cell proliferation of fibroblasts after 24 h of incubation with increasing concentrations of RSV or DHS. Cell cycle analysis of RSV-treated cells showed that this agent induced a significant accumulation ($p \leq 0.01$) of cells in S-phase with a consequent reduction in the number of cells in G1 phase (G1 = 39.9, S = 35.05, G2 + M = 25.1; G1 = 47, S = 39.55, G2 + M = 13.45 at 15 and 30 μM, respectively), with respect to the cell cycle distribution of control cells (G1 = 60.7, S = 22.55, G2 + M = 16.75). Under the same conditions, DHS showed an accumulation of cells in G1 phase ($p \leq 0.05$), and a concomitant decrease in S-phase cell population, at all the concentrations used (G1 = 71.45, S = 14.91, G2 + M = 13.63 at 7.5 μM; G1 = 69.89, S = 15.76, G2 + M = 14.35 and G1 = 73.53, S = 11.08, G2 + M = 15.37 at 15 and 30 μM, respectively). To further investigate the effect on cell cycle, DNA replication was assessed by BrdU incorporation assay. Fig. 3C shows representative image of BrdU-positive nuclei of fibroblasts treated with 30 μM RSV as compared with 7.5 μM DHS. Fig. 3B shows that the percentage of BrdU-positive nuclei was significantly increased (50%), in cells treated with the highest concentration of resveratrol, as compared to control cells (15%). It is important to note that most of the BrdU-positive nuclei showed an immunofluorescence pattern that is typical of early S-phase, indicating that RSV inhibited DNA replication at the initial steps (Locatelli et al., 2005). Instead, DHS significantly inhibited BrdU incorporation already at a concentration as low as 2.5 μM (7% compared to 21% of control cells, $p < 0.05$). These results clearly confirm that DHS induces a G1 arrest, preventing cells to enter S phase and start DNA synthesis. Similar data were obtained in the human breast adenocarcinoma cell line MCF7 (not shown). The inhibitory effect on cell cycle progression induced by both RSV or DHS was reversible, since the percentage of cells in S phase returned to the control value (data not shown) at 24 and 72 h after their removal, respectively.

### 3.3. DHS inhibits DNA pol δ activity and DNA replication in "in vitro" assays

The results obtained by BrdU incorporation in fibroblasts indicated that DHS prevented cells from entering S phase, while RSV delayed S-phase progression. As previously demonstrated (Stivala et al., 2001), the accumulation of cells in early S-phase induced by resveratrol was a consequence of a direct inhibition of DNA synthesis. To verify whether the analogue acted similarly to the natural compound, the ability of DHS to inhibit DNA synthesis was investigated both in vitro with purified proteins, and in a cell-free DNA replication system. As previously observed (Stivala et al., 2001; Locatelli et al., 2005), RSV at 20 μM inhibited the activity of both DNA pol α and pol δ to a similar extent (62% and 52%, respectively), whereas DHS, at the same concentration, significantly inhibited DNA pol δ (by about 45%), but not pol α (Fig. 4A). At this concentration both compounds did not affect pol β activity. To further confirm the capacity of the two compounds to inhibit DNA polymerase activity, a cell-free replication assay was performed on S-phase synchronized nuclei from HeLa cells. Following

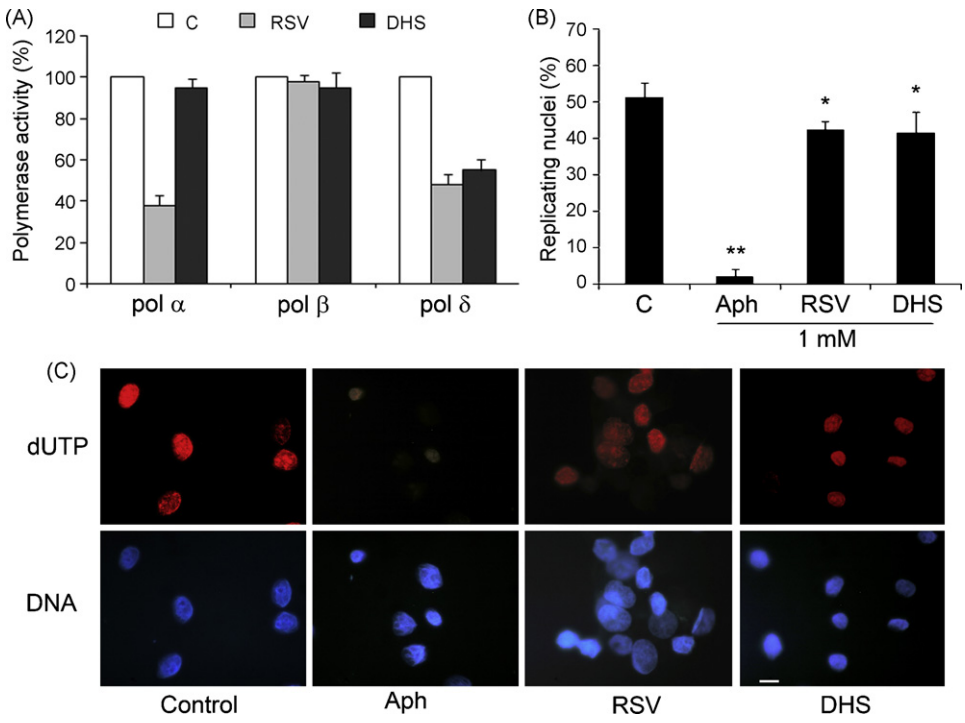


**Fig. 4.** Effect of RSV and DHS on DNA synthesis in vitro and in cell-free system replication assay. DNA synthesis performed in vitro (A) by purified pol α, pol β, and pol δ. Assays were performed in the presence of 20 μM of each inhibitor to be tested. DNA polymerase activity was expressed as percentage of the control reaction without inhibitor which was 0.8 pmol × $min^{-1}$ for pol α and 0.6 pmol × $min^{-1}$ for pol δ and taken as 100%. (B) Quantitation of the percentages of nuclei replicating in cytosolic extract of S-phase HeLa cells in the absence (control) and in the presence of 1 mM RSV or its analogue DHS. Representative field of nuclei (C) from thymidine-arrested HeLa cells incubated in S-phase cytosol, or in the presence of Aphidicolin (Aph), RSV, and DHS. Nuclei were isolated from cells arrested at the beginning of S-phase by double-blocking of thymidine and incubated in S-phase cytosol, as described in Section 2. Nuclear DNA replication is visualized by Texas red-conjugated streptavidin (red signal) and DNA by Hoechst staining (blue signal). Scale bar 10 μM. $^{*}p \leq 0.05$, $^{**}p \leq 0.01$.

incubation in S-phase HeLa cytosol, approximately 60% of intact nuclei efficiently initiated DNA replication, as assessed by incorporation of biotinylated dUTP (Fig. 4B and C); RSV and its analogue inhibited DNA replication by about 17 and 18.9% ($p < 0.05$), respectively, while a total inhibition was exerted by Aphidicolin ($p < 0.01$), a well-known pol δ inhibitor (Fig. 4C). It should be also noted that for both compounds, fluorescence intensity of replicating nuclei appeared less intense than those of control nuclei.

### 3.4. RSV and its analogue DHS induce a similar expression pattern of cell cycle regulatory specific genes

To further investigate whether the different effect on cell cycle progression by the two stilbenic molecules was due to unscheduled expression of specific cell cycle regulatory proteins, the expression of series of human genes was analyzed by using a cell cycle pathway-specific gene array. Fig. 5 shows a representative image of the different gene expression pattern after cell treatment with each compound, as compared to the untreated sample. Changes included mainly up-regulation of genes related to the cell cycle control, with the exception of the transcription factors E2F4 that resulted up-regulated (by about twofold) in control cells, compared to RSV- and DHS-treated cells. Instead, comparable results were obtained in LF1 treated with RSV or DHS, where up-regulation of the cdk inhibitors p21, p27, p16, p15, and p19 were found. Similarly, cyclins A2, B2, C, D2, D3, G1, G2 and H were over-expressed in both treated samples, together with the cell cycle regulatory proteins CDC20, CDC25A, CDC6, CDK2, CDK7, E2F2, PCNA, PRC1, MCM2. Interestingly, an increased RNA level of genes implicated in cell cycle checkpoints, such as ATM, CHK1, CKSB1, MRE11A, HUS1, NBS1 were also detected (Fig. 5). The analysis of the phosphorylation level of Chk1 ($Ser^{317/345}$), downstream targets of ATR/ATM, was analyzed by Western blotting. The results (Supplementary Fig. 1) showed that, as compared with asynchronous control cells, a clear signal was detected only in cells treated with RSV, and in UV-irradiated HeLa cells (positive control). In order to investigate whether p21-dependent G1 arrest in response to DHS was related to the presence of DNA damage, the phosphorylation on $Ser^{139}$ (γ-H2AX) was also assessed. A percentage of about 16% of γ-H2AX positive cells were found both in RSV- and DHS-treated samples (Supplementary Fig. 2), while no signal was observed in untreated samples.

### 3.5. DHS induces changes in cell cycle regulatory proteins

To establish whether RSV and DHS impaired cell cycle progression with a different molecular mechanism, the specific induction of cell cycle regulatory molecules, such as the CDK inhibitors p27, p21, and p16, together with cyclins D1, E, and A, were evaluated by Western blot analysis. In addition, the retinoblastoma (pRb) and p53 protein levels were investigated. Fig. 6A shows that RSV did not induce any significant change in the levels of the CDK inhibitors analyzed, in agreement with our previous results (Stivala et al., 2001), whereas they appeared up-regulated in fibroblasts treated with DHS at the highest concentration, as compared to parental cells. In DHS-treated fibroblasts, p21 and p16 protein levels were about three and twofold higher, respectively, than those observed in control samples as evaluated by densitometry and normalization on actin levels. No significant changes in cyclins E levels were observed (data not shown), whereas changes in the phosphorylation level of cyclin D1 were observed only in DHS-treated cells, together with the complete disappearance of cyclin A bands (Fig. 6A and B). In addition, the slower migrating forms of pRb were more abundant in cells treated with RSV, as compared to control and DHS-treated fibroblasts, which showed mainly the faster migrat-

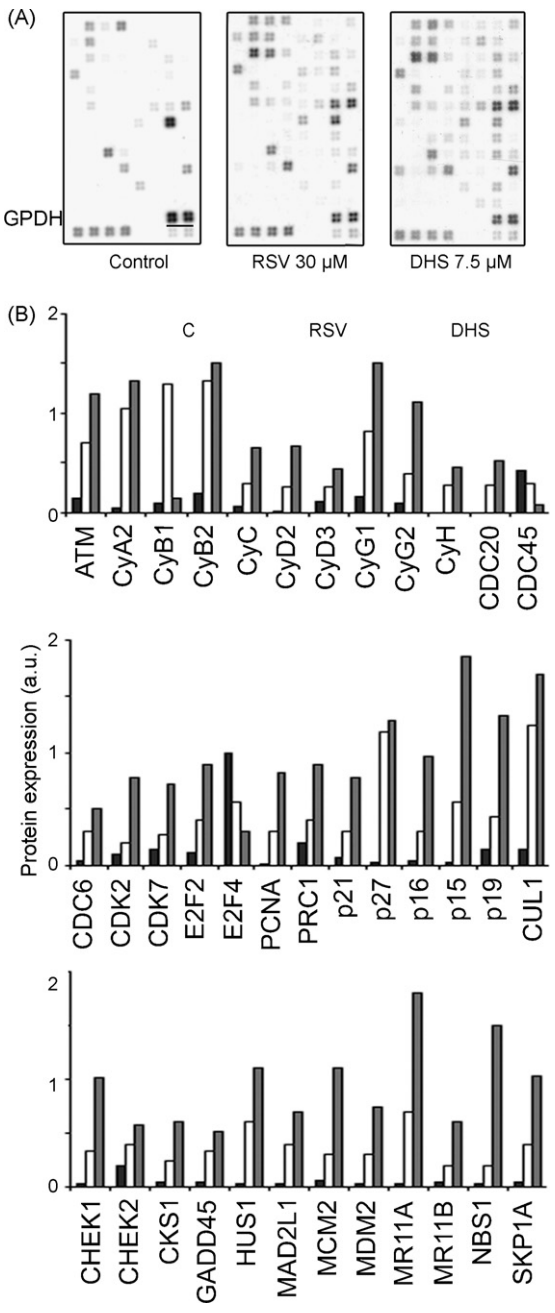


**Fig. 5.** Effect of RSV and DHS on cell cycle gene expression of human fibroblasts. Representative cell cycle gene arrays (A), and quantitative analysis (B) of gene expression in untreated LF1 fibroblasts or in cells treated for 24 h with RSV (30 μM) and its analogue DHS (7.5 μM). Glyceraldehyde-3-phosphate dehydrogenase (GPDH) gene expression was considered as internal loading control.

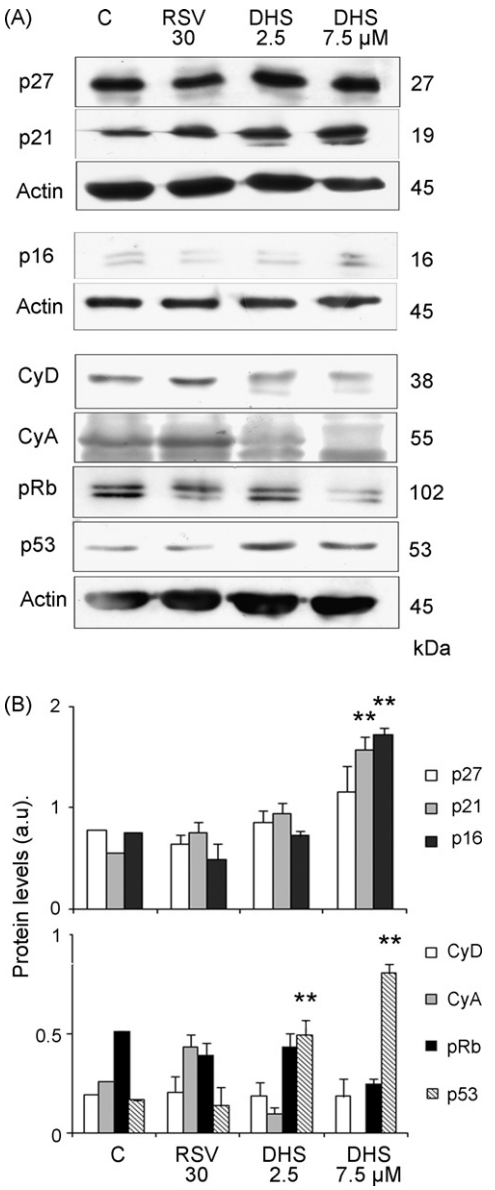


**Fig. 6.** Effect of RSV and DHS on cell cycle regulatory protein levels of human fibroblasts. Western blot analysis (A) performed in LF1 human fibroblasts after 24-h treatment with RSV (30 μM) or DHS (2.5 and 7.5 μM). Actin was determined as loading control. Densitometric analysis (B) of the p27, p21, p16, cyclins D and A, pRB and p53 immunoreactivity normalized to the internal loading control.

ing forms. At highest DHS concentration, cells showed lower levels of both hyper- and hypo-phosphorylated forms of pRb. Finally, p53 protein levels resulted unmodified in RSV-treated cells, whereas a significant increase (by about three and fivefold) was detected in both DHS-treated samples.

### *3.6. DHS treated cells show lower levels of chromatin-bound MCM2 than RSV*

In order to better explore the basis underlying the G1 cell cycle imbalance induced by DHS, the chromatin recruitment of MCM2 protein, typically occurring in G1 phase, was next investigated. Western blot analysis of soluble and chromatin-bound MCM2 showed that this protein was recruited in DHS-treated cells to a similar extent than control sample (Fig. 7A), whereas a significant increase of the band corresponding to MCM2 was observed in cells treated with RSV. A similar MCM2 recruitment was observed by flow cytometry. Fig. 7B shows the dot plots of MCM2 immunofluorescence versus DNA content in control cells, and in fibroblasts treated for 24 h with 30 μM RSV, or with 2.5 and 7.5 μM DHS, respectively. Immunofluorescence levels of MCM2 increase from early to late G1 phase, reaching the highest amount at the G1/S phase transition, before declining during S phase. Accumulation of LF1 fibroblasts at the G1/S phase transition was evident in cells treated with RSV, while after DHS treatment, cells did not show (either at 2.5 or at 7.5 μM) any significant difference in MCM2 recruitment, as compared to control cells, confirming the results obtained by Western blot. To better understand how RSV or DHS-treated cells moved through cell cycle, LF1 fibroblasts were synchronized in G0 phase by serum starvation for 72 h (SS), and

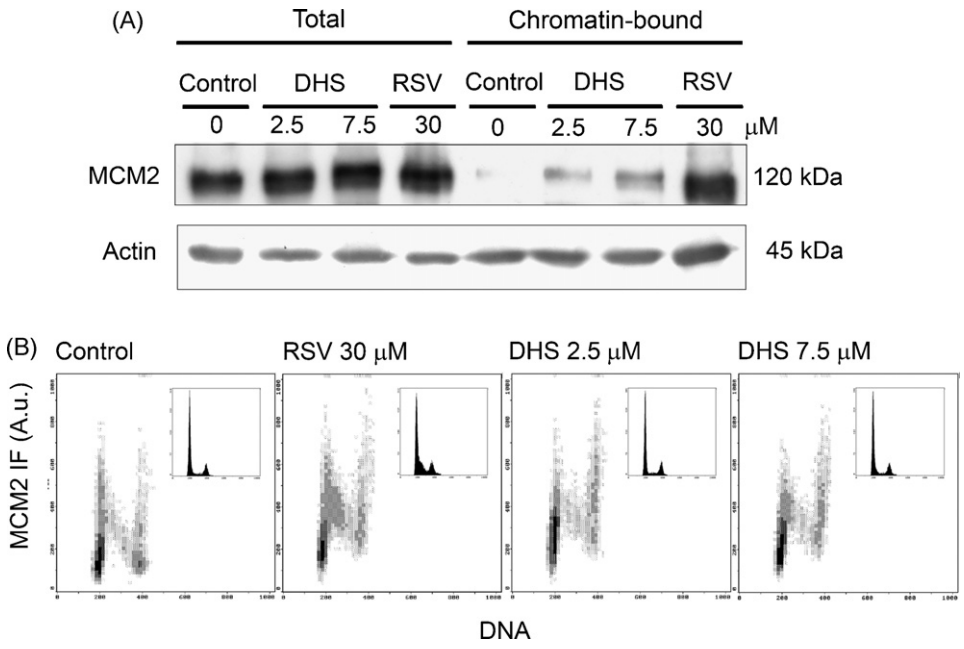


**Fig. 7.** Effect of RSV and DHS on the MCM2 recruitment on to chromatin. Western blot analysis of total and chromatin-bound MCM2 (A) in LF1 fibroblasts after 24-h treatment with RSV (30 μM) or DHS (2.5 and 7.5 μM). Actin was determined as loading control. Two-parameter dot plots (B) of chromatin-bound MCM2 immunofluorescence versus DNA content in control cells, and in fibroblasts treated for 24 h with 30 μM RSV, or 2.5 and 7.5 μM DHS. Determination of detergent-insoluble form of MCM2 was performed as described in Section 2.

then released in the complete medium containing the two stilbenic compounds. Fig. 8 shows the dot plots of MCM2 immunofluorescence versus DNA content in G0-arrested cells (72 h SS (b)), untreated cells (control (c) and (d)), and in cells treated for 24 or 48 h with 30 μM RSV ((e) and (f)), or with 2.5 ((g) and (h)) and 7.5 μM ((i) and (l)) DHS, respectively. The results showed that LF1 fibroblasts in the presence of RSV, and more remarkably in the presence of DHS, progressed through S phase at a slower rate than control cells. In fact, an accumulation of fibroblasts at G1/S phase transition was evident after 24 h of RSV treatment, while at 48 h cells were blocked mainly at S/G2 phase transition. DHS-treated cells showed a different behaviour, with a significant increase in the number of cells in G1 phase at 24 h, as indicated also by the high MCM2 immunofluorescence levels typical of cells in G1; after 48 h of DHS-treatment, cells started to enter S-phase at the lowest concentration, but not at 7.5 μM, where cells were still blocked at G1 phase, with few S-phase events.

### 3.7. DHS does not inhibit DNA replication in p21-null cells

To confirm the involvement of p21 in the cell cycle impairment induced by DHS, experiments were performed in human Tert-fibroblasts in which the p21 gene was deleted by homologous recombination (Brown et al., 1997). For this purpose, $p21^{+/+}$ and $p21^{-/-}$ cells were treated with RSV or DHS under the same conditions used for primary LF1 cells, and DNA synthesis was assessed by

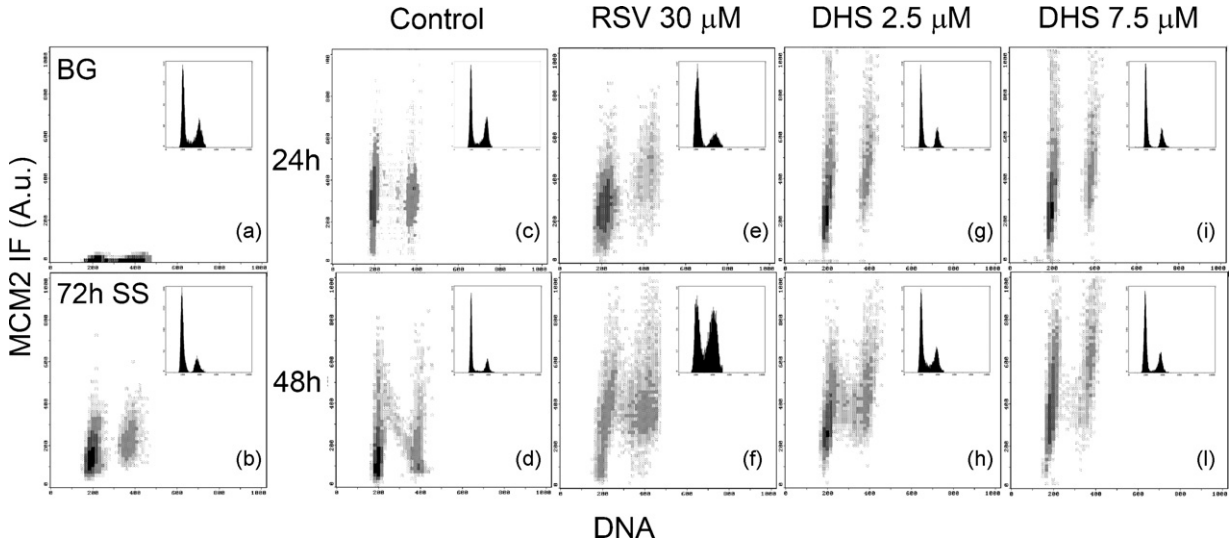


**Fig. 8.** Effect of RSV and DHS on the MCM2 recruitment on to chromatin. Two-parameter dot plots of chromatin-bound MCM2 immunofluorescence versus DNA content in control cells synchronized by 72 h of serum starvation (b), and in the absence ((c) and (d)) or in the presence of RSV ((e) and (f)) and DHS ((g)–(l)), after 24 or 48 h of release from serum starvation. Determination of detergent-insoluble form of MCM2 was performed by immunostaining and flow cytometric analysis, as described under Section 2. BG = background.

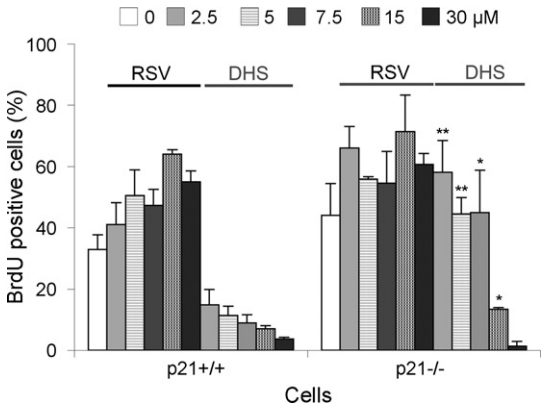


**Fig. 9.** Effect of RSV and DHS on $p21^{+/+}$ and $p21^{-/-}$ human Tert-fibroblasts. DNA synthesis was evaluated by BrdU incorporation in $p21^{+/+}$ and $p21^{-/-}$ human Tert-fibroblasts seeded on coverslips, treated with increasing concentration of RSV and DHS, and processed as described in Section 2. All results are expressed as mean ± SD from three independent experiments. $^{*}p < 0.05$, $^{**}p < 0.01$ versus $p21^{+/+}$ cells at the same conditions.

BrdU incorporation. Fig. 9 shows that, similarly to LF1 primary cells, in the $p21^{+/+}$ cells RSV induced a marked increase (from 10 to 30%) in the number of BrdU-positive nuclei, whereas DHS significantly inhibited (by about 50%) BrdU incorporation, already at a concentration as low as 2.5 μM. Compared with the parental cells, p21-null fibroblasts showed a similar behaviour after RSV-treatment, in contrast DHS did not induce any inhibition in BrdU incorporation in p21-null cells up to 7.5 μM; only at the highest concentration of 15 and 30 μM it started to inhibit DNA synthesis.

## 4. Discussion

Disruption of the normal regulation of cell cycle progression and division are important events in the development of cancer. Targeting of these critical events represents the goal of cancer chemoprevention through dietary agents, mainly identified in fruits and vegetables (Pervaiz, 2003; Bauer and Sinclair, 2006; Meeran and Katiyar, 2008). We have previously investigated the mechanisms underlying the antiproliferative effects of the wine microcomponent resveratrol (Stivala et al., 2001). In the present study we have investigated and compared the biological properties of DHS with those of resveratrol. Short-term cell toxicity, together with clonogenic efficiency assay, showed that DHS was more potent than RSV at inhibiting cell growth, in primary human fibroblasts. A weak cytotoxic effect was found at concentration as high as 90 μM for RSV and 15 μM for DHS. However, Trypan blue dye exclusion test (data not shown) evidenced the absence of cell death in the presence of each compound up to 60 μM, supporting that the results obtained with the MTT assay reflect mainly cell growth inhibition rather than loss of cell viability in this range. The relationship between the presence of 4′-hydroxyl group and antiproliferative as well as cytotoxic effect has already been reported (Stivala et al., 2001; Billack et al., 2008, Fan et al., 2009). Accordingly, our findings demonstrate that the two-hydroxyl groups on 4- and 4′-positions of the stilbenic backbone increase its cytostatic and antiproliferative activity in fibroblasts. Further experiments to investigate cell cycle progression revealed that the superior antiproliferative activity of DHS over RSV was associated with several differences in their mechanism. First, DHS induced predominantly G1 arrest, as determined by cell cycle analysis and BrdU incorporation. In contrast, RSV induced an accumulation of cells at the beginning of S-phase. The cytostatic effect of RSV may be attributed to a decreased DNA synthesis, given that inhibition of BrdU incorporation was previously found (Fontecave et al., 1998; Hsieh and Wu, 1999; Stivala et al., 2001), and its ability to inhibit DNA pol α and δ or DNA elongation was confirmed by in vitro assays. Interestingly, DHS showed an inhibitory effect on DNA pol δ in the in vitro assays, but it did not affect pol α activity. In fact, its effect on cell cycle progression occurred markedly in G1 phase, as also indicated by the absence of cyclin A, a reduction of total Rb levels, and by the high CDC6 together with undetectable CDC45 protein levels (Supplementary Fig. 3).

In contrast, increased cyclin A and CDC45 protein levels and highly phosphorylated forms of pRb were observed in RSV-treated cells, indicating progression through the G1 restriction point, and accumulation in early S phase. Consistent with these results, recruitment of chromatin-bound MCM2 was detected, both by Western blot and cytofluorimetric analysis, in RSV-treated cells, compared to DHS-treated samples.

It is well known that a number of checkpoints exist within the mammalian cell cycle, which ensure that cell division proceeds normally. The transition from G1 to S-phase is strictly regulated by sequential formation, activation and inactivation of a series of cell cycle regulatory molecules (Li and Brooks, 1999). At the expression level, no significant difference were observed between RSV or DHS-treated cells, but an increasing RNA level of several regulatory cell cycle genes, such as CDKs inhibitors, cyclins, and several genes involved in checkpoints, were detected compared to control cells. However, at the protein level, only DHS-treatment was associated with an increase in p21 and p53 protein levels. The involvement of p21 CDK inhibitor in the mechanism of action of DHS was clearly demonstrated by the absence of the antiproliferative effect in p21-null cells. Although a p21-based mechanism was demonstrated for RSV in previous reports (Hsieh et al., 1999a; Hudson et al., 2007), we did not observe a significant change in this protein and in its transcriptional regulator p53 in RSV-treated normal fibroblasts. Interestingly, RSV, but not DHS, activated the S-phase checkpoint as shown by the presence of phosphorylation on $Ser^{317}$ of Chk1 protein, but both compounds induced phosphorylation of histone H2AX, indicating some level of DNA damage. It was previously found that DHS exhibit in vitro, in the presence of Cu (II) ions, a prooxidant, DNA damaging activity higher than resveratrol (Zheng et al., 2006). In our system, failure to detect single or double-breaks by Comet test (data not shown), suggest that the extent of DNA damage was very low. Thus, the observed p21-dependent G1-arrest after DHS treatment could be explained by an eventual formation of small amount of oxidative products (Zheng et al., 2006; Hadi et al., 2007). In contrast, stalled replication forks could underlie S-phase accumulation in

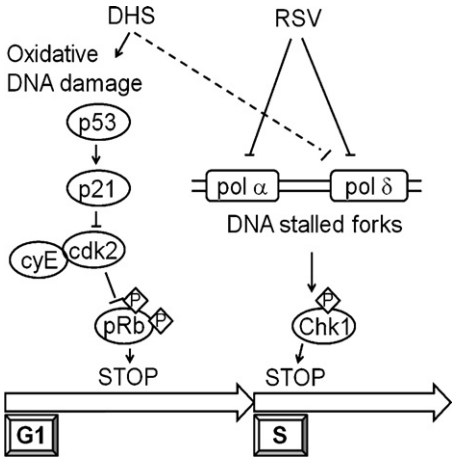


**Scheme 1.** Proposed mechanisms for cell cycle inhibition by DHS and RSV.

RSV-treated cells. A schematic model related to the pathways targeted by each compound has been proposed in Scheme 1. In conclusion, our results suggest that the two-hydroxyl groups on 4- and 4′-positions of the stilbenic backbone enhance the antiproliferative effect and introduce additional targets in the mechanism of action of the resveratrol analogue. Further studies are now in progress to clarify its effect in cancer cells, since DHS might be a promising agent for chemoprevention. Compared with normal cells, cancer cells have been shown to contain elevated levels of copper (Ebara et al., 2000), and may be more sensitive to subject to electron transfer with antioxidants to generate ROS (Zeisel and Salganik, 1999). Therefore, DNA damage induced by stilbenes in the presence of copper may be an important pathway through which cancer cells can be killed while normal cells survived.

## Acknowledgements

This work was supported by a MIUR grant (PRIN 2005/2005063915) and work in G. Maga laboratory was partially supported by an AIRC-Associazione Italiana Ricerca sul Cancro Investigator Grant. The Authors wish to thank J.M. Sedivy (Brown University, Providence, RI) for providing LF1, h-Tert $p21^{+/+}$ and $p21^{-/-}$ fibroblasts. Maccario C. is also acknowledged for technical assistance.

## Appendix A. Supplementary data

Supplementary data associated with this article can be found, in the online version, at doi:10.1016/j.biocel.2009.08.005.

## References

Alessi F, Quarta S, Savio M, Riva F, Rossi L, Stivala LA, et al. The cyclin-dependent kinase inhibitors Olomoucine and Roscovitine arrest human fibroblasts in G1 phase by specific inhibition of CDK2 kinase activity. Exp Cell Res 1998;245:8–18.

Arichi H, Kimura Y, Okuda H, Baba K, Kozawa M, Arichi S. Effects of stilbene components of the roots of Polygonum cuspidatum on lipid metabolism. Chem Pharm Bull 1982;30:1766–70.

Balan KV, Wang Y, Chen SW, Chen JC, Zheng LF, Yang L, et al. Proteasome-independent down-regulation of estrogen receptor-alpha (ERalpha) in breast cancer cells treated with 4,4'-dihydroxy-trans-stilbene. Biochem Pharmacol 2006;72:573–81.

Barger JL, Kayo T, Vann JM, Arias EB, Wang J, Hacker TA, et al. A low dose of dietary resveratrol partially mimics caloric restriction and retards aging parameters in mice. PLoS ONE 2008;3(6):e2264.

Bauer JA, Sinclair DA. Therapeutic potential of resveratrol: the in vivo evidence. Nat Rev 2006;5:493–506.

Baur JA, Pearson KJ, Price NL, Jamieson HA, Lerin C, Kalra A, et al. Resveratrol improves health and survival of mice on a high-calorie diet. Nature 2006;16(444(7117)):337–42.

Billack B, Radkar V, Adiabouah C. In vitro evaluation of the cytotoxic and antiproliferative properties of resveratrol and several of its analogs. Cell Mol Biol Lett 2008;13:553–69.

Brown JP, Weiw W, Sedivy JM. Bypass of senescence after disruption of p21cip/waf gene in normal diploid human fibroblasts. Science 1997;277:831–4.

Cai YJ, Fang JG, Ma LP, Yang L, Liu ZL. Inhibition of free radical-induced peroxidation of rat liver microsomes by resveratrol and its analogues. Biochim Biophys Acta 2003;1637:31–8.

Cheng JC, Fang JG, Chen WF, Zhou B, Yang L, Liu ZL. Structure-activity relationship studies of resveratrol and its analogues by the reaction kinetics of low density lipoprotein peroxidation. Bioorg Chem 2006;34:142–57.

Ebara M, Fukuda H, Hatano R, Saisho H, Nagato Y, Suzuki K, et al. Relationship between copper, zinc and metallothionein in hepatocellular carcinoma and its surrounding liver parenchyma. J Hepatol 2000;33:415–22.

Fan GJ, Liu XD, Qian YP, Shang YJ, Li XZ, Dai F, Fang JG, Jin XL, Zhou B. 4,4′-dihydroxy-trans-stilbene, a resveratrol analogue, exhibited enhanced antioxidant activity and cytotoxicity. Bioorg Med Chem 2009;17:2360–5.

Fang H, Tong W, Shi LM, Blair R, Perkins R, Branham W, et al. Structure-activity relationships for a large diverse set of natural, synthetic, and environmental estrogens. Chem Res Toxicol 2001;14:280–94.

Fang JG, Lu M, Chen ZH, Zhu HH, Li Y, Yang L, et al. Antioxidant effects of resveratrol and its analogues against the free-radical-induced peroxidation of linoleic acid in micelles. Chemistry 2002;8:4191–8.

Fontecave M, Lepoivre M, Elleingand E, Gerez C, Guittet O. Resveratrol, a remarkable inhibitor of ribonucleotide reductase. FEBS Lett 1998;412:277–9.

Frankel EN, Waterhouse AL, Kinsella JE. Inhibition of human LDL oxidation by resveratrol. Lancet 1993;341:1103–4.

Goldberg DM, Hahn SE, Parkes JG. Beyond alcohol: beverage consumption and cardiovascular mortality. Clin Chem Acta 1995;237:155–87.

Hadi SM, Bhat SH, Azmi AS, Hanif S, Shamim U, Ullah MF. Oxidative breakage of cellular DNA by plant polyphenols: a putative mechanism for anticancer properties. Semin Cancer Biol 2007;17:370–6.

Hain R, Bieseler B, Kindl H, Schroder G, Stocker R. Expression of a stilbene synthase gene in Nicotiana tabacum results in synthesis of the phytoalexin resveratrol. Plant Mol Biol 1990;15:325–35.

Howitz KT, Bitterman KJ, Cohen HY, Lamming DW, Lavu S, Wood JG, et al. Small molecule activators of sirtuins extended Saccharomyces cerevisiae lifespan. Nature 2003;425:191–6.

Hsieh T, Juan G, Darzynkiewicz Z, Wu JM. Resveratrol increases nitric oxide synthase, induces accumulation of p53 and p21waf1/cip1 and suppresses bovine pulmonary artery endothelial cell proliferation by perturbing progression through S and G2. Cancer Res 1999a;59:2596–601.

Hsieh T, Wu JM. Differential effects on growth, cell cycle arrest, and induction of apoptosis by resveratrol in human prostate cancer cell lines. Exp Cell Res 1999;249:109–15.

Hsieh TC, Burfeind P, Laud K, Bacher JM, Traganos F, Darzynkiewicz Z, et al. Cell cycle effects and control of gene expression by resveratrol in human breast carcinoma cell lines with different metastatic potentials. Int J Oncol 1999b;15:245–52.

Hudson TS, Hartle DK, Hursting SD, Nunez NP, Wang TTY, Young HA. Inhibition of prostate cancer growth by muscadine grape skin extract and resveratrol through distinct mechanisms. Cancer Res 2007;67:8396–405.

Jang DS, Kang BS, Ryu SY, Chang IM, Min KR, Kim Y. Inhibitory effects of resveratrol analogs on unopsonized zymosan-induced oxygen radical production. Biochem Pharmacol 1999;57:705–12.

Jang M, Cai L, Udeani GO, Slowing KV, Thomas CF, Beecher CWW, et al. Cancer chemopreventive activity of resveratrol, a natural product derived from grapes. Science 1997;275:218–20.

Kerry NL, Abbey M. Red wine and fractionated phenolic compounds prepared from red wine inhibit low density lipoprotein oxidation in vitro. Atherosclerosis 1997;135:93–102.

Kimura Y, Okuda H, Arichi S. Effects of stilbenes on arachidonate metabolism in leukocytes. Biochim Biophys Acta 1985;834:275–8.

Klinge CM, Wickramasinghe NS, Ivanova MM, Dougherty SM. Resveratrol stimulates nitric oxide production by increasing estrogen receptor alpha-Src-caveolin-1 interaction and phosphorylation in human umbilical vein endothelial cells. FASEB J 2008;22:2185–97.

Kotha A, Sekharam M, Cilenti L, Siddiquee K, Khaled A, Zervos AS, et al. Resveratrol inhibits Src and Stat3 signaling and induces the apoptosis of malignant cells containing activated Stat3 protein. Mol Cancer Ther 2006;5:621–9.

Krude T. Initiation of human DNA replication in vitro using nuclei from cells arrested at an initiation-competent state. J Biol Chem 2000;275:13699–707.

Langcake P, Pryce RJ. A new class of phytoalexins from grapevines. Experientia 1977;33:151–2.

Li JM, Brooks G. Cell cycle regulatory molecules (cyclins, cyclin-dependent kinases and cyclin-dependent kinase inhibitors) and the cardiovascular system. Eur Heart J 1999;20:406–20.

Locatelli GA, Savio M, Forti L, Shevelev I, Ramadan K, Stivala LA, et al. Inhibition of mammalian DNA polymerases by resveratrol: mechanism and structural determinants. Biochem J 2005;389:259–68.

MacCarrone M, Lorenzon T, Guerrieri P, Finazzi Agrò A. Resveratrol prevents apoptosis in K562 cells by inhibiting lipoxygenase and cyclooxygenase activity. Eur J Biochem 1999;265:27–34.

Meeran SM, Katiyar SK. Cell cycle control as a basis for cancer chemoprevention through dietary agents. Front Biosci 2008;13:2191–202.

Mgbonyebi OP, Russo J, Russo IH. Antiproliferative effect of synthetic resveratrol on human breast epithelial cells. Int J Oncol 1998;12:865–9.

Milne JC, Lambert PD, Schenk S, Carney DP, Smith JJ, Gagne DJ, et al. Small molecule activators of SIRT1 as therapeutics for the treatment of type 2 diabetes. Nature 2007;450:712–6.

Mosmann T. Rapid colorimetric assay for cellular growth and survival: application to proliferation and cytotoxicity assays. J Immunol 1983;65:55–63.

Pace-Asciak CR, Hahn S, Diamandis EP, Soleas G, Goldberg DM. The red wine phenolics trans-resveratrol and quercetin block human platelet aggregation and eicosanoid synthesis: implications for protection against coronary heart disease. Clin Chim Acta 1995;235:207–19.

Pace-Asciak CR, Rounova O, Hahn S, Diamandis EP, Goldberg DM. Wines and grape juices as modulators of platelet aggregation in healthy human subjects. Clin Chim Acta 1996;246:163–82.

Pervaiz S. Resveratrol: from grapevines to mammalian biology. FASEB J 2003;17:1975–85.

Rotondo S, Rajtar G, Manarini S, Celardo A, Rotilio D, de Gaetano G, et al. Effect of trans-resveratrol, a natural polyphenolic compound, on human polymorphonuclear leukocyte function. Brit J Pharmacol 1998;123:1691–9.

Scovassi AI, Prosperi E. Analysis of proliferating cell nuclear antigen (PCNA) associated with DNA excision repair sites in mammalian cells. Methods Mol Biol 2006;314:457–75.

Soleas GJ, Diamandis EP, Goldberg DM. Resveratrol: a molecule whose time has come? And gone? Clin Biochem 1997;30:91–113.
Stivala LA, Savio M, Carafoli F, Perucca P, Bianchi L, Maga G, et al. Specific structural determinants are responsible for the antioxidant activity and the cell cycle effects of resveratrol. J Biol Chem 2001;276: 22586–94.
Sun NJ, Woo SH, Cassady JM, Snapka RM. DNA polymerase and topoisomerase II inhibitors from Psoralea corylifolia. J Nat Prod 1998;61:362–6.
Szewczuk LM, Forti L, Stivala LA, Penning TM. Resveratrol is a peroxidase-mediated inactivator of COX-1 but not COX-2: a mechanistic approach to the design of COX-1 selective agents. J Biol Chem 2004;279(21):22727–37.
Zeisel SH, Salganik RI. Antioxidants and nutrition support. Curr Opin Clin Nutr Metab Care 1999;2:1–3.
Zheng LF, Wei QY, Cai YJ, Fang JG, Zhou B, Yang L, Liu ZL. DNA damage induced by resveratrol and its synthetic analogues in the presence of Cu (II) ions: mechanism and structure-activity relationship. Free Radic Biol Med 2006;41:1807–16.